MOLECULAR AND CELLULAR BIOLOGY, Apr. 1988, p. 1489–1497
0270-7306/88/041489-09$02.00/0

Vol. 8, No. 4

Molecular Analysis of Hybrid Dysgenesis-Induced Derivatives of a P-Element Allele at the *vg* Locus

JIM A. WILLIAMS,* SITA S. PAPPU, AND JOHN B. BELL

Department of Genetics, University of Alberta, Edmonton, Alberta, Canada T6G 2E9

Received 27 October 1987/Accepted 6 January 1988

Secondary and tertiary derivatives of a P-element insertion allele at the vestigial (*vg*) locus were induced by hybrid dysgenesis. The derivatives were characterized by Southern analyses and, in four cases, by DNA sequencing. The alterations found were P-element internal deletions, deletions of the insert and/or adjacent *vg* region DNA, or novel insertions of P-element sequences into existing P-element inserts. The relatively high frequency of secondary insertions into P-element sequences observed herein is unusual, since secondary insertions have seldom been recovered in other dysgenic screens. The effects of the alleles on *vg* expression were determined. The results are consistent with a model in which the insertions disrupt *vg* gene expression by transcriptional interference.

Hybrid dysgenesis mediated by P elements is a powerful tool for studying gene expression in *Drosophila melanogaster*. It is induced in the progeny of crosses between P-cytotype males and M-cytotype females, but not in the reciprocal cross. P strains contain multiple copies of chromosomal P elements, while M strains lack functional P elements (27). Dysgenic crosses cause mutations due to P-element insertions into genes or imprecise excisions from genes with preexisting P-element sequences. The functional P element is a 2.9-kilobase (kb) transposon which encodes a transposase that is required for transposition (17, 26). Most P elements in a P strain are smaller than the 2.9-kb element and are derived from this element by an internal deletion (24). P elements have 31-base-pair (bp) terminal repeats on each flank which are required for transposition (14), and 8 bp of chromosomal DNA is duplicated at the insertion site (24). The internally deleted P elements are unable to produce their own transposase, but they are mobilized when supplied with transposase produced by complete P elements (28, 32). Transpositional activity occurs only under dysgenic conditions, since P strains also encode a repressor which prevents transposition in P-cytotype flies. It is unknown what the structure of the repressor is or exactly how it works, but it appears to be encoded by P-element sequences (for a review, see reference 6).

P-element mutagenesis can be used to produce primary or secondary mutants at a locus. Primary mutants are usually insertions of P-element sequences into a gene and are particularly useful in facilitating the initial cloning of genes. A variety of loci have been cloned in this manner (1, 18, 31). Secondary mutants arise when preexisting P-element alleles are induced to undergo further dysgenic activity (at rates as high as 10^{-2} to 10^{-3}) (24, 34). The secondary mutants are often revertants, but they may also be more extreme derivatives of the original allele. They have been extensively studied at the rudimentary (34), RPII215 (30, 35), and yellow loci (3). Secondary mutants have been shown to be due to either precise or imprecise P-element excisions (3, 24, 30, 34, 35), internal deletions within the resident P element (4, 30, 34), deletion of DNA adjacent to the resident P element (4, 34), or inversions with a breakpoint within the P element (7, 34). Thus, P elements within a locus can be potent mutators. The examples described above all involve P elements inserted into the promoter region of the respective genes, which appears to be a preferential target among recovered P-element insertions (for a review, see reference 15).

Here, we report results of an analysis of secondary and tertiary P-element-induced mutations at the vestigial (*vg*) locus. The *vg* gene is required for normal wing formation. Strong *vg* alleles cause extensive cell death in the third instar wing imaginal disks, resulting in complete loss of the adult wing margin (10). However, weak *vg* alleles cause less severe wing loss, and various phenotypic gradations exist between strong and weak *vg* alleles. Thus, secondary *vg* alleles can be selected which are only subtly different from the parent allele. The *vg* gene has been cloned by P-element tagging. The region has been partially characterized at the DNA level, and an adult *vg*-specific transcript has been identified (J. A. Williams and J. B. Bell, submitted for publication). The primary P-element-induced mutation was shown to be due to P-element sequences inserted into the 3′ region of the gene. A series of secondary and tertiary derivatives of this *vg* allele were induced by further hybrid dysgenesis. These alleles were examined by DNA cloning and DNA sequence analysis. The results provide additional corroborating examples of previously described types of secondary P-element-induced mutations and, in addition, identify an unusual form of secondary event. The results also provide evidence for models of transcriptional interference as a mechanism by which P-element insertions disrupt target gene expression.

MATERIALS AND METHODS

***D. melanogaster* stocks and culturing.** *D. melanogaster* cultures were grown at 24°C and maintained on a synthetic medium (22). Recombination mapping was performed by crossing the relevant *vg* flies to a multiply marked second chromosome stock (*al dp b pr cn vg c a px bw mr sp*/In [2L] Cy In [2R] Cy) obtained from J. Kennison, and by backcrossing F_1 mutant *vg*/marker chromosome females to vg^{BG} males. On testing, the vg^+ progeny were all found to have only the proximal flanking markers, which indicates that all of the derived *vg* alleles mapped proximal to the *vg* allele of the marker chromosome. Southern hybridization analyses were used to confirm that the *vg* allele on the marker chromosome was the vg^{BG} allele (a strong *vg* allele obtained

* Corresponding author.

from Bowling Green Stock Center, Bowling Green, Ohio) physically characterized previously (Williams and Bell, submitted).

Materials. Restriction enzymes and other DNA-modifying enzymes were obtained from Bethesda Research Laboratories, Inc. (Gaithersburg, Md.) or Pharmacia Fine Chemicals (Piscataway, N.J.) and were used according to the instructions of the manufacturers. All radioisotopes were purchased from New England Nuclear Corp. (Boston, Mass.). Oligolabeled probes were labeled with [α-^{32}P]dCTP (3,000 Ci/mmol), and RNA probes were labeled with [α-^{32}P]UTP (3,000 Ci/mmol), while for DNA sequencing [α-^{32}P]dATP (800 Ci/mmol) was used. The RP49 clone was a gift from M. Rosbach.

DNA manipulations. Culturing and storage of bacteria or lambda phage, preparation of DNA, and plasmid subcloning were performed by standard methods (19). Genomic *D. melanogaster* DNA for Southern hybridizations and genomic libraries was prepared by the method of Ish-Horowicz et al. (13) and repurified by spermine precipitation (12).

Genomic libraries. The $vg^{21\text{-}3}$ and $vg^{21\text{-}4\text{-}Rev}$ libraries were constructed in strain EMBL-3 by the method of Frischauf et al. (9). *Bam*HI-restricted *D. melanogaster* DNA was electrophoresed in 0.4% agarose gels, and 18 to 20 kb-fragments were retained by electroelution onto dialysis membranes, ethanol precipitated, and suspended in 5 μl of TE buffer. Vector DNA (4 μl; 1 μg/2 μl) was added, ligated, and packaged as described previously (19). The $vg^{21\text{-}4}$, $vg^{21\text{-}7}$, and $vg^{21\text{-}7\text{-}Rev}$ libraries were constructed in λGT10. The genomic DNA was digested with *Eco*RI and size selected on 1% agarose gels as described above. Purification, ligation, and packaging were done as indicated above. EMBL-3 libraries were plated on NM-539, and λGT10 libraries were plated on C600 HfL. Genomic libraries were transferred to biodyne membranes (Pall) and prepared for hybridization by standard methodologies.

Southern and Northern hybridizations. All gels for Southern or Northern hybridization analysis were blotted onto membranes (Genescreen Plus; E. I. du Pont de Nemours & Co., Inc., Wilmington, Del.) by using the capillary blot protocol recommended by the manufacturer. RNA was extracted, purified by oligo(dT) chromatography, and electrophoresed on 1.5% formaldehyde gels as described by Gietz and Hodgetts (11). For Northern gels, 4 μg of poly(A)$^+$ RNA per lane was used, while for Southern gels 5 μg of DNA per lane was used. Size markers for Southern gels were obtained by mixing the digestion products of pπ25.1 treated with a variety of enzymes and calibrated by comparison with the known sequence (24). Hybridization conditions for all plaque lifts, Southern hybridizations, and DNA-probed Northern hybridizations were those of Klessig and Berry (16). Southern and DNA-probed Northern hybridization probes were washed according to specifications for the Genescreen Plus membranes. DNA probes were made from restriction fragments resolved on low-melting-point agarose gels and oligolabeled by the method of Feinberg and Vogelstein (8). RNA probes for Northern hybridizations were prepared from restriction fragments cloned into Bluescribe (Vector Cloning Systems) by using the transcription protocol of Melton et al. (20), and their methods for hybridization and washing of RNA-probed Northern hybridization probes were also used. The prehybridization and hybridization temperatures were 65°C.

DNA sequencing. All sequencing was performed by the dideoxy method (29) from inserts in M13mp18 and M13mp19. Since all of the P-element mutants analyzed in this study had alterations within a 200-bp genomic *Sst*I-*Pst*I fragment (see Fig. 6), the sequencing was limited to this region. The Oregon-R (OR-R) sequence was determined by sequencing both strands of the 200-bp *Sst*I-*Pst*I fragment. The vg^{21} insert was characterized by sequencing both strands of the *Pst*I-*Hin*dIII, *Hin*dIII-*Sca*I, and *Sca*I-*Sst*I fragments, and single strands of the *Pst*I-*Sst*I fragment to establish overlap at the *Hin*dIII and *Sca*I sites (see Fig. 6). Both strands of the following subclones (see Fig. 6) were sequenced to map the lesions in the vg^{21} derivatives: $vg^{21\text{-}4}$ *Hin*dIII-*Sca*I, *Sca*I-*Sst*I, and *Pst*I-HindIII; $vg^{21\text{-}7}$, *Pst*I-*Hin*dIII (one strand) and *Hin*dIII-*Sst*I; $vg^{21\text{-}4\text{-}Rev}$, *Sst*I-*Sca*I and *Sca*I-*Pst*I; $vg^{21\text{-}7\text{-}Rev}$, *Pst*I-*Hin*dIII (one strand), *Hin*dIII-*Sal*I, *Sal*I-*Sca*I, and *Sca*I-*Sst*I.

RESULTS

Induction of vg^{21} derivatives by hybrid dysgenesis. Molecular cloning of the *vg* locus has facilitated a detailed analysis of the DNA lesions associated with several mutants and the identification of an adult *vg*-specific transcript (Williams and Bell, submitted). A map of the *vg* region is shown in Fig. 1, and the alterations associated with three *vg* alleles are indicated. A region of 19 kb (coordinates 0 to +19) was defined which is required for normal *vg* function. The *vg* locus was cloned by using a hybrid dysgenesis-induced P-element allele. This *vg* allele (henceforth called vg^{21}) was caused by the insertion of an internally deleted P element into a OR-R wild-type chromosome. The phenotype of vg^{21} is cryptic (i.e., homozygous wild type), but it shows a weak *vg* phenotype when heterozygous with a strong *vg* allele (i.e., vg^{BG}).

The cryptic phenotype of vg^{21} lends itself to the selection of more extreme hybrid dysgenesis-induced derivatives. When initially isolated, the vg^{21} stock was backcrossed to a M-cytotype strain (vg^{BG}) for several generations to stabilize the allele in an M cytotype. For this study, a vg^{21} P-cytotype strain was reestablished by multiple passages of the vg^{21} chromosome through a P-cytotype balancer strain derived from the π2 stock (a strong P-cytotype stock from W. Engels). A dysgenic cross was then performed (Fig. 2). A total of 32 *vg* phenotype flies were isolated from the 1.5 × 10^4 F_2 flies that were screened. A control cross of the same strains under nondysgenic conditions yielded no *vg* flies among 10^4 that were screened, demonstrating that the 32 *vg* mutants described above were induced by hybrid dysgene-

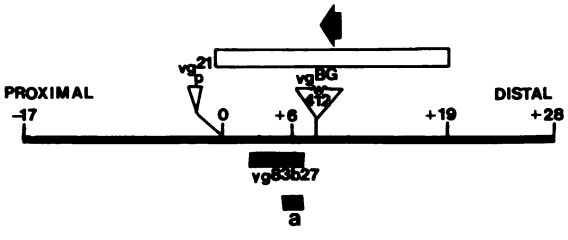

FIG. 1. The *vg* region of *D. melanogaster*. The alterations associated with the three *vg* alleles cited in this study are indicated. vg^{21} is a 650-bp insertion of an internally deleted P element, while vg^{BG} is a 9-kb insertion of a 412 element. vg^{83b27} is a deletion whose limits are shown by the black bar. The open bar denotes the region defined to be essential for *vg* function. The arrow indicates the direction of *adult-specific vg* gene transcription. The data are from Williams and Bell (submitted). The solid bar labeled with the letter a represents the fragment which was used as a probe for the Northern hybridization presented later.

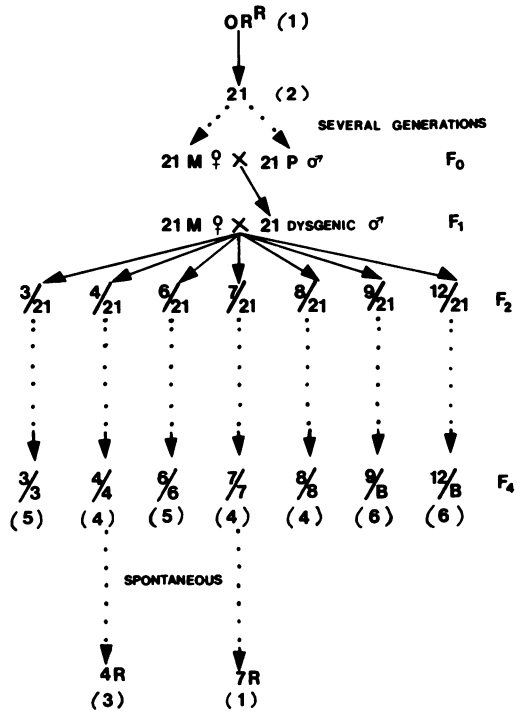

FIG. 2. Flow chart of the isolation of dysgenic derivatives of vg^{21}. The vg^{21} allele was induced by hybrid dysgenesis in OR-R flies as described previously (Williams and Bell, submitted). The F_2 wing-defective mutants ($vg^{21\text{-}m}/vg^{21}$) were made homozygous by backcrossing single flies to vg^{21} (M cytotype) and self-crossing the $vg^{21\text{-}m}/vg^{21}$ offspring to isolate $vg^{21\text{-}m}/vg^{21\text{-}m}$ progeny. In the case of $vg^{21\text{-}9}$ and $vg^{21\text{-}12}$, the homozygotes were lethal, so stocks of these were established and maintained by using a balancer chromosome. Stocks of $vg^{21\text{-}4\text{-}Rev}$ and $vg^{21\text{-}7\text{-}Rev}$ were established as described in the text. The vg^{21} derivative alleles are designated above the slash as, for example, 3 = $vg^{21\text{-}3}$, while M is the M cytotype, P is the P cytotype, and B is the balancer chromosome. The wing phenotype of each allele is indicated by a number in parentheses below or beside the genotypic abbreviations. The numbering system proceeds from weak to strong alleles, in which 1 is the wild-type allele and 6 is a null allele.

sis. A very high level of sterility was observed among these F_2 *vg* mutants, as only 12 of them were fertile. Of these, seven that were known to be of independent origin were chosen for further study, and stocks of these were established. Preliminary genetic analysis indicated that all seven derivatives of vg^{21} were indeed *vg* alleles.

Analysis of two lethal vg^{21} derivatives. The only two vg^{21} derivatives from the present screen that were homozygous lethal were $vg^{21\text{-}9}$ and $vg^{21\text{-}12}$. Both of these alleles behaved genetically as *vg* null alleles. Since these alleles are unconditional lethal alleles, while null *vg* alleles show escaper flies (Williams and Bell, submitted), this lethality was not likely *vg* specific. Southern hybridization analyses of *Sal*I-restricted DNA from flies heterozygous for the respective lethal alleles and each of two different *vg* alleles are shown in Fig. 3A. The results indicate that the $vg^{21\text{-}12}$ derivative has a deletion encompassing the region defined by the two probes that were used, while this region was not deleted from the $vg^{21\text{-}9}$ derivative. The rationale for this conclusion is based on the observation that the vg^{21} chromosome yielded a 23-kb *Sal*I DNA fragment which was split into two fragments in $vg^{21\text{-}3}$ (described below). Since only the vg^{21}-specific band was seen in the $vg^{21\text{-}12}/vg^{21}$ lane (Fig. 3A) and only the $vg^{21\text{-}3}$-specific bands were seen in the $vg^{21\text{-}12}/vg^{21\text{-}3}$ lane (Fig. 3A) (when either probe was used), then the $vg^{21\text{-}12}$ chromosome must have a deletion that at least includes the +6 to −7 region. In Fig. 3, probe C also did not recognize $vg^{21\text{-}12}$-specific restriction fragments (data not shown). Results of this analysis do not preclude the possibility that $vg^{21\text{-}12}$ is associated with other more complex rearrangements. However, the demonstrated deletion of the *vg* region DNA is sufficient to be responsible for the *vg* null phenotype observed, so we examined this allele no further.

Similar logic was used to interpret the results presented in Fig. 3B. In this case, the $vg^{21\text{-}9}$ allele was heterozygous with either vg^{21} or $vg^{21\text{-}3}$; and DNA from these flies was restricted with *Xho*I, *Pst*I, or *Eco*RI and analyzed by Southern hybridization. Since vg^{21} and $vg^{21\text{-}3}$ exhibited different-sized restriction fragments for each of the three digests (see below), the presence of $vg^{21\text{-}9}$-specific restriction fragments was easily detected. In Fig. 3B, panels 1 and 2 demonstrate that $vg^{21\text{-}9}$ has a deletion which removes the probe C region but not the probe D region. In Fig. 3B, panel 3 shows further characterization of this deletion by use of *Eco*RI and *Pst*I Southern blots. The results are consistent with the idea that $vg^{21\text{-}9}$ has a deletion of 2 kb which removes the vg^{21} insert and *vg* region DNA both proximal and distal to it, including the entire 0.7-kb *Eco*RI fragment within which the P element was inserted.

Analysis of viable vg^{21} derivatives. Five of the vg^{21} derivatives ($vg^{21\text{-}3}$, $vg^{21\text{-}4}$, $vg^{21\text{-}6}$, $vg^{21\text{-}7}$, and $vg^{21\text{-}8}$) were homozygous viable. Genomic Southern analysis of *Pst*I- or *Eco*RI-restricted genomic DNA from these mutant strains was performed by using probes from throughout the cloned region (positions −18 to +28). The only alterations found were in the same genomic *Eco*RI and *Pst*I fragments within which the vg^{21} insert was located. The $vg^{21\text{-}7}$ and $vg^{21\text{-}8}$ derivatives had deletions within the fragments, while $vg^{21\text{-}3}$ and $vg^{21\text{-}6}$ were complex, with additional DNA inserted into the fragments (data not shown). The $vg^{21\text{-}4}$ derivative contained a small deletion (<50 bp) within the same region described above.

To genetically determine whether the physical alterations associated with the vg^{21} derivatives were associated with the more extreme *vg* phenotypes that were selected, intragenic recombination analyses were done (see above). The vg^{21} allele has already been genetically mapped in relation to vg^{BG} (Williams and Bell, submitted) and is positioned approximately 0.028 map units centromere proximal to vg^{BG}. The vg^{21} derivatives also mapped closely proximal to vg^{BG}. One vg^{+} recombinant was isolated for each of $vg^{21\text{-}3}$, $vg^{21\text{-}4}$, $vg^{21\text{-}6}$, and $vg^{21\text{-}7}$ of 7,730, 2,660, 9,508, and 8,898 flies scored, respectively, from each cross. These results indicate that the physical lesions observed with the four vg^{21} derivatives described above are probably the causative lesions of the more extreme *vg* phenotypes, since they mapped genetically to the same general location where the lesions were observed.

Further physical analyses helped to define more precisely the alterations associated with these vg^{21} derivatives. Since DNA from the $vg^{21\text{-}3}$ allele releases two *Eco*RI fragments (data not shown), the *Bam*HI DNA fragment from positions −11 to +6 was cloned for this derivative, to ensure that the entire insert was obtained (see above). The cloned fragment was mapped by restriction enzyme analysis, and gels with various restriction digests were Southern blotted and probed with pπ25.1 (24) to detect P-element sequences (data not shown). The results (Fig. 4) indicate that the original small vg^{21} insert became a 2.6-kb insert at the same site. All the

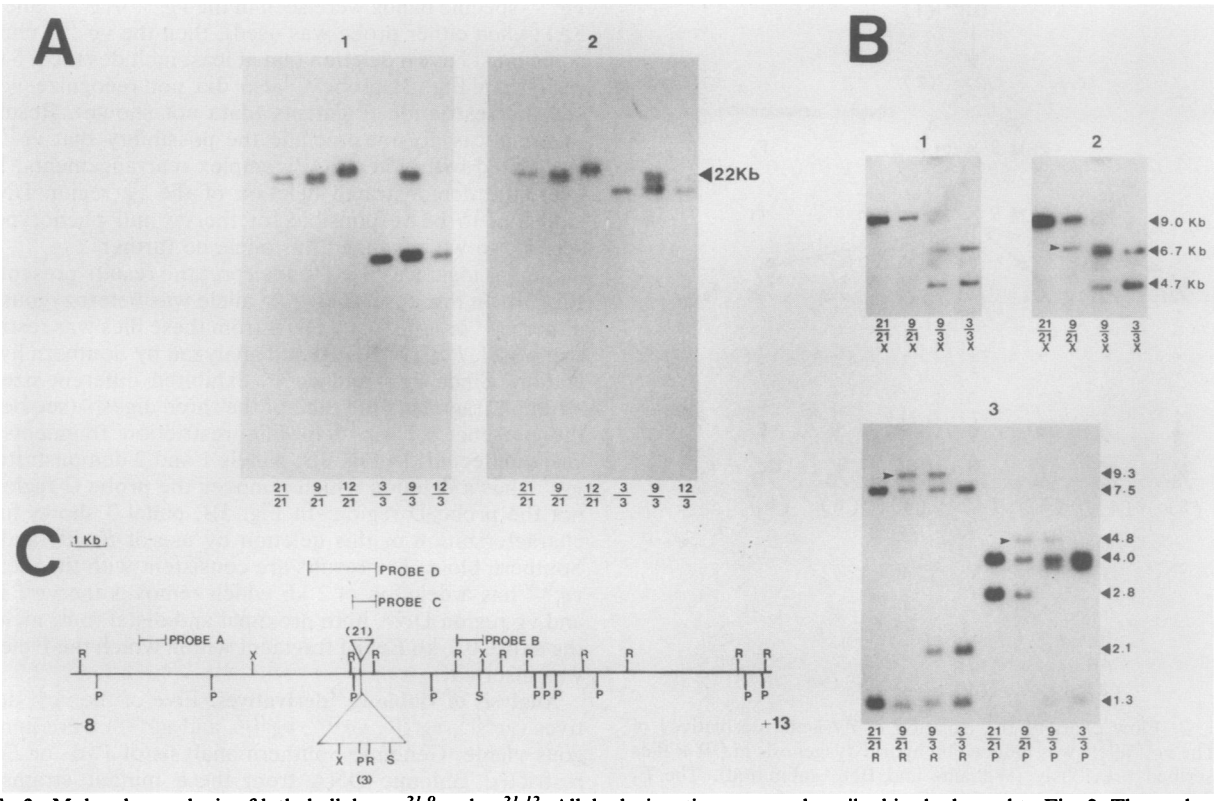

FIG. 3. Molecular analysis of lethal alleles vg^{21-9} and vg^{21-12}. Allele designations are as described in the legend to Fig. 2. The probes used for the Southern blots in panels A and B are indicated in panel C. (A) Southern blots of *Sal*I-restricted DNA from flies of the indicated genotypes were made; blot 1 was hybridized with probe A, while blot 2 was hybridized with probe B. The *Sal*I band in lane 12/21 was larger than expected, probably because excess DNA was loaded into that lane. (B) Southern blots with DNA from flies of the indicated genotypes were hybridized with either probe C (blot 1) or probe D (blots 2 and 3). Arrowheads within the gels indicate novel fragments seen in the vg^{21-9} lanes. (C) Restriction map of the region with the indicated probes. The vg^{21} insert and the vg^{21-3} derivative insert are also shown, with the extra restriction sites in the vg^{21-3} insert indicated. Restriction enzyme designations are as follows: S, *Sal*I; P, *Pst*I; R, *Eco*RI; X, *Xho*I.

restriction fragments within the insert hybridized to P-element sequences, and the restriction map matched perfectly with that of a complete P element (24), except for a small internal deletion near the 3′ end. Thus, vg^{21-3} seems to be a novel type of conversion-like event of the small vg^{21} insert into a much larger insert through an as yet unknown process. The nature of vg^{21-6} has not yet been rigorously determined, but it appears to be similar in type to vg^{21-3}. Since these alleles are of independent origin, this indicates that the secondary insertion of DNA in vg^{21-3} is not an isolated event.

The affected *Eco*RI fragments of vg^{21-4} and vg^{21-7} were cloned (see above) and mapped by further restriction endonuclease analyses. The vg^{21-7} derivative was shown to have deleted most of the DNA between the *Hin*dIII and *Sst*I sites of vg^{21}, while a small (about 40 bp) deletion between the *Hin*dIII and *Sst*I sites was detected in the vg^{21-4} derivative (data not shown). The exact nature of the molecular lesions in vg^{21-4} and vg^{21-7} was determined by DNA sequencing of vg^{21} and these two derivatives (see above). The results (Fig. 5) indicate that the vg^{21} mutation is due to a 687-bp insertion of an internally deleted P element into the 200-bp OR-R *Pst*I-*Sst*I restriction fragment. A single-base insertion in the 5′-terminal repeat was present in the vg^{21} insert, as compared with the published P-element sequence (24). Since, to the best of our knowledge, no other examples of base changes in the terminal repeats have been characterized, it is difficult to predict the effects on transposition. The sequence of the *Pst*I-*Sst*I OR-R fragment indicates that vg^{21} is a clean insert which has a novel 9-bp duplication of OR-R DNA flanking the insert (Fig. 5). It is possible that the extra base in the terminal repeat may affect transposition, causing a 9-bp duplication. Conversely, there may have been an 8-bp duplication followed by insertion of one nucleotide at the junction. The sequencing of the two vg^{21} derivatives shows that in vg^{21-7} 529 bp of DNA was deleted (to within 14 bp of the 3′ end of the vg^{21} P-element insert), while in vg^{21-4} 36 bp of *vg* locus DNA immediately adjacent to but entirely

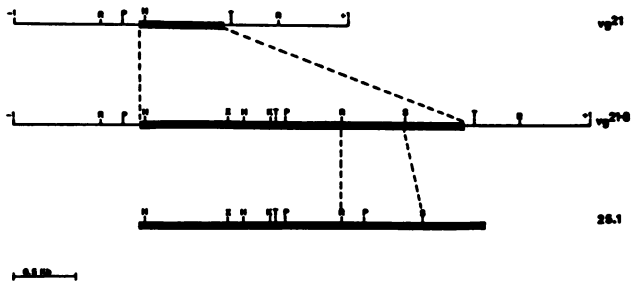

FIG. 4. Restriction map analysis of vg^{21} and vg^{21-3}. The P-element insertions of the respective alleles are indicated by solid bars, and flanking DNAs are indicated by thin lines. The restriction map of pπ25.1, a complete P element (24), is shown at the bottom of the figure. Restriction enzymes are abbreviated as described in the legend to Fig. 3; other abbreviations: H, *Hin*dIII; T, *Sst*I; K, *Kpn*I.

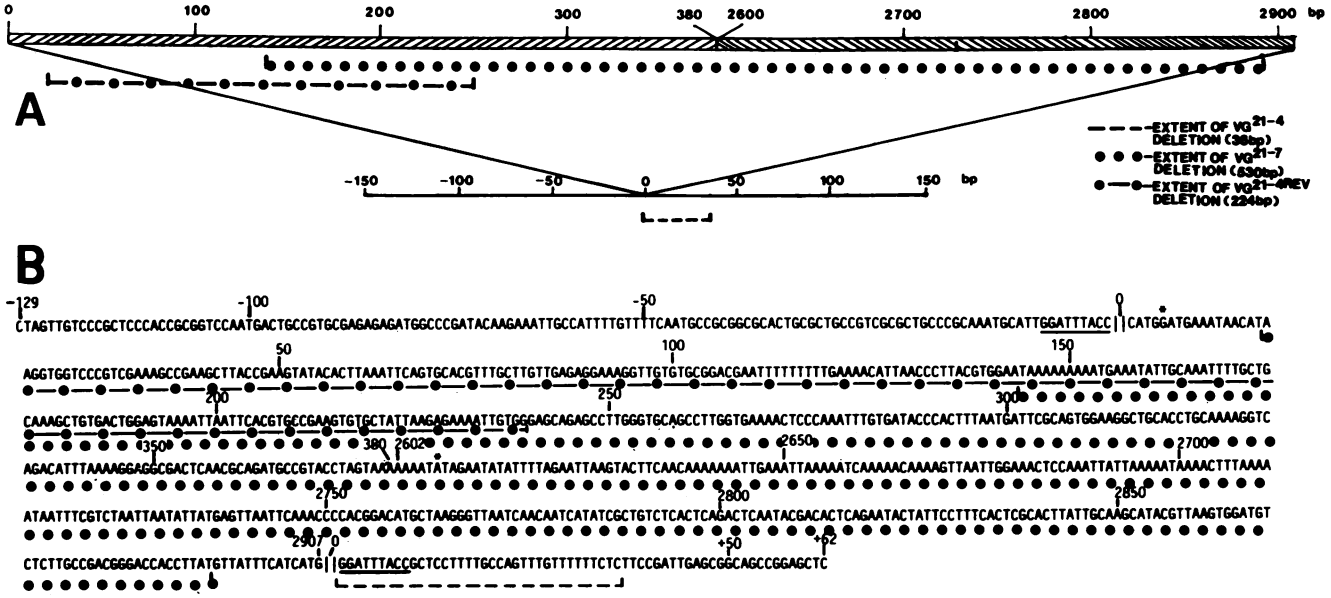

FIG. 5. DNA sequence analysis of vg^{21} and three derivatives. (A) Schematic diagram of the vg^{21} insert with the extent of the DNA deletions in three vg^{21} derivatives as indicated. (B) Sequence of the vg^{21} insert, numbered as described by O'Hare and Rubin (24), with the indicated flanking *D. melanogaster* genomic DNA from the *vg* region. Symbols for the three vg^{21} derivatives, with the relevant sequences deleted, are as described for panel A. The $vg^{21\text{-}4\text{-}Rev}$ derivative also contained the $vg^{21\text{-}4}$ deletion, which was expected since $vg^{21\text{-}4\text{-}Rev}$ was derived from $vg^{21\text{-}4}$. The 9 bp duplicated at the insertion site are underlined. Asterisks denote extra vases in the P-element inserts which differ from the published sequence (24). The $vg^{21\text{-}4\text{-}Rev}$ derivative has three bases (GAT; data not shown) inserted at the internal deletion end point, while $vg^{21\text{-}7}$ has two bases inserted at the breakpoint (GG; data not shown). This type of alteration has been observed before (24, 30). The genomic *Pst*I site is at position −139 (data not shown), while the genomic *Sst*I site is at position +62.

outside the vg^{21} insert was deleted. Both derivatives retained the extra base in the 5′-terminal repeat. The 9-bp duplication was retained in $vg^{21\text{-}7}$, but in $vg^{21\text{-}4}$ the 3′ portion was deleted.

Analysis of $vg^{21\text{-}4\text{-}Rev}$. A spontaneous partial revertant ($vg^{21\text{-}4\text{-}Rev}$) was isolated from the $vg^{21\text{-}4}$ stock (Fig. 2) which exhibited strap-like wings in homozygotes instead of the more extreme *vg* wing phenotype of $vg^{21\text{-}4}$. Figure 6A shows a Southern blot hybridization of *Pst*I-restricted DNA from flies homozygous for $vg^{21\text{-}4}$, $vg^{21\text{-}4\text{-}Rev}$, and the original $vg^{21\text{-}4}$ stock (which contained a mixture of $vg^{21\text{-}4}$ and $vg^{21\text{-}4\text{-}Rev}$ flies). The pure $vg^{21\text{-}4}$ and $vg^{21\text{-}4\text{-}Rev}$ stocks were selected from the original $vg^{21\text{-}4}$ stock by either repeated selection for *vg* extreme or *vg* weak phenotypes or selection of weak and extreme *vg* phenotypes from flies heterozygous over various other *vg* alleles (labeled 1 and 2, respectively, in Fig. 6A). The results indicate that the mixed stock contains two aberrant *Pst*I bands, one of which was the same size as the $vg^{21\text{-}4}$ band seen above (Fig. 3) and one of which was 200 bp smaller. DNA from both homozygous $vg^{21\text{-}4\text{-}Rev}$ stocks was associated with this smaller band. The −11 to +6 *Bam*HI fragment, which contained the affected region, was used to clone the $vg^{21\text{-}4\text{-}Rev}$ allele (see above). Restriction digests of the insert showed that the only alteration in the region was the 200-bp deletion described above. A schematic representation of the generation of this derivative allele, starting from vg^{21}, is shown in Fig. 6A. Since the revertant was allelic to *vg* and associated with a DNA alteration in the same region as all of the previous derivative alleles characterized above, we feel that this alteration is the lesion responsible for the revertant phenotype. The insert region of $vg^{21\text{-}4\text{-}Rev}$ was sequenced to localize the deletion endpoints precisely; these results are shown in Fig. 5.

Analysis of $vg^{21\text{-}7\text{-}Rev}$. A spontaneous phenotypic revertant ($vg^{21\text{-}7\text{-}Rev}$) was isolated from the $vg^{21\text{-}7}$ stock (Fig. 2), which

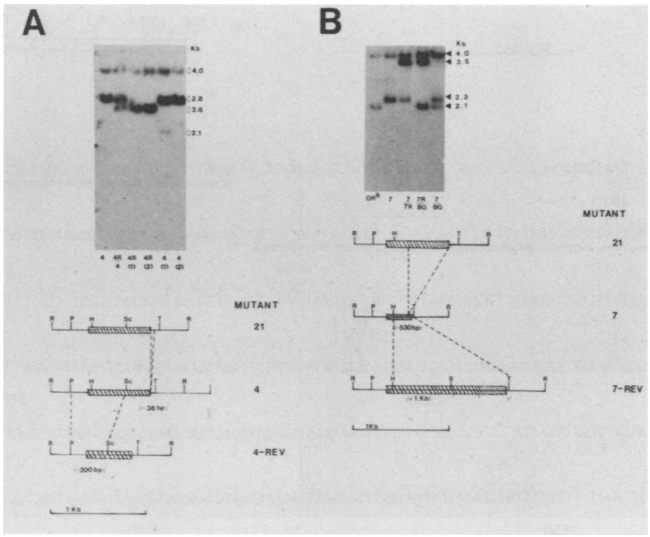

FIG. 6. Southern hybridization analyses and interpretative flow diagrams of $vg^{21\text{-}4\text{-}Rev}$ and $vg^{21\text{-}7\text{-}Rev}$. (A and B) Southern blots of *Pst*I-restricted DNA from flies of the indicated genotypes hybridized with probe C from Fig. 3. Strain designations are as described in the legend to Fig. 2, and BG is vg^{BG}. The designations 1 and 2 indicate independent lines of $vg^{21\text{-}4}$ and $vg^{21\text{-}4\text{-}Rev}$ established by two different selection methods. At the bottom of each panel are flow diagrams indicating the physical alterations that took place, proceeding from vg^{21} through to either $vg^{21\text{-}4\text{-}Rev}$ or $vg^{21\text{-}7\text{-}Rev}$. The cross-hatched bars denote P-element sequences. Restriction enzyme designations and restriction maps are as described in the legend to Fig. 4. The alterations shown for $vg^{21\text{-}4\text{-}Rev}$ and $vg^{21\text{-}7\text{-}Rev}$ were derived from DNA restriction analyses and DNA sequencing of clones of these alleles.

almost completely complements vg^{BG}. Results of Southern hybridization analysis of *Pst*I-digested DNA from $vg^{21\text{-}7\text{-}Rev}$ are shown in Fig. 6B and indicate that this derivative allele, surprisingly, is associated with a further insertion into the $vg^{21\text{-}7}$ insert and is not the expected deletion of $vg^{21\text{-}7}$ P-element sequences. Further Southern blot analyses indicated that this alteration was within the same *Eco*RI fragment that contained the other vg^{21} derivatives discussed above (data not shown). The altered *Eco*RI fragment was cloned and restriction mapped (see above). These results are summarized in Fig. 6B, and a schematic representation of the generation of this allele from the vg^{21} allele is shown. The $vg^{21\text{-}7\text{-}Rev}$ insert was sequenced, and the comparison of this sequence with the parent insert is given in Fig. 7. The $vg^{21\text{-}7\text{-}Rev}$ allele resulted from a novel insertion of a 1.1-kb P element into the $vg^{21\text{-}7}$ insert. The data are most consistent with the $vg^{21\text{-}7\text{-}Rev}$ derivative resulting from a P-element integration into $vg^{21\text{-}7}$ at the 3′ end (at base 100) and a homologous recombination with the $vg^{21\text{-}7}$ insert at the 5′ end. For this reason, the exact integration site at the 5′ end is not shown in Fig. 7; the P-element sequences of either possible origin ($vg^{21\text{-}7}$ or $vg^{21\text{-}7\text{-}Rev}$) are indicated. No base changes were seen in the portion of $vg^{21\text{-}7}$ which was retained in $vg^{21\text{-}7\text{-}Rev}$ (Fig. 7). The 9-bp duplication and the extra base in the 5′-terminal repeat were also retained in $vg^{21\text{-}7\text{-}Rev}$.

***vg* transcript analysis.** Adult *vg*-specific transcripts have been identified (Williams and Bell, submitted). To examine how the series of P-element inserts affect adult *vg* expression, adult poly(A)$^+$ RNA was prepared from the vg^{BG}, vg^{83b27}, OR-R, and homozygous viable P-element-induced alleles reported here and was examined by Northern blot analysis (Fig. 8) by using the *vg*-specific probe identified in Fig. 1. No transcripts were detected in the vg^{83b27} lane, which demonstrates that the transcripts are *vg* specific since vg^{83b27} is a homozygous deletion of the probe region (see Fig. 1). The blot was subsequently rehybridized with a RP49 probe (23) to control for differences in the amount of RNA in each lane. The results indicate that the mutants affect the level of adult *vg* transcripts without altering the size. The *vg* transcript levels in the lane with $vg^{21\text{-}3}$ did not appear reduced relative to those in the lane with vg^{21} (Fig. 8). This was unexpected, since $vg^{21\text{-}3}$ is a more severe *vg* allele than vg^{21}. However, since we did not sequence $vg^{21\text{-}3}$, it is possible that this allele is more severe due to structural alterations in the *vg* region DNA flanking the $vg^{21\text{-}3}$ insert (i.e., like $vg^{21\text{-}4}$). Comparison of *vg* transcript levels with the RP49 control indicated that both $vg^{21\text{-}4\text{-}Rev}$ and $vg^{21\text{-}7\text{-}Rev}$ have enhanced *vg* transcription compared with vg^{21}, $vg^{21\text{-}3}$, and $vg^{21\text{-}7}$; $vg^{21\text{-}4}$ has transcript levels comparable to those of vg^{21}, $vg^{21\text{-}3}$, and $vg^{21\text{-}7}$ (data not shown).

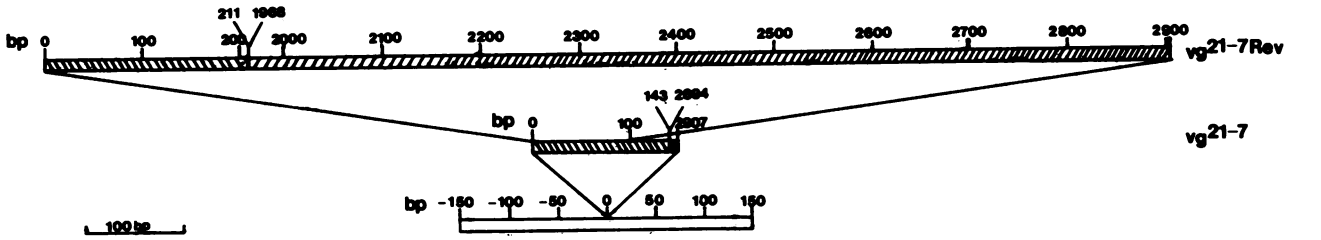

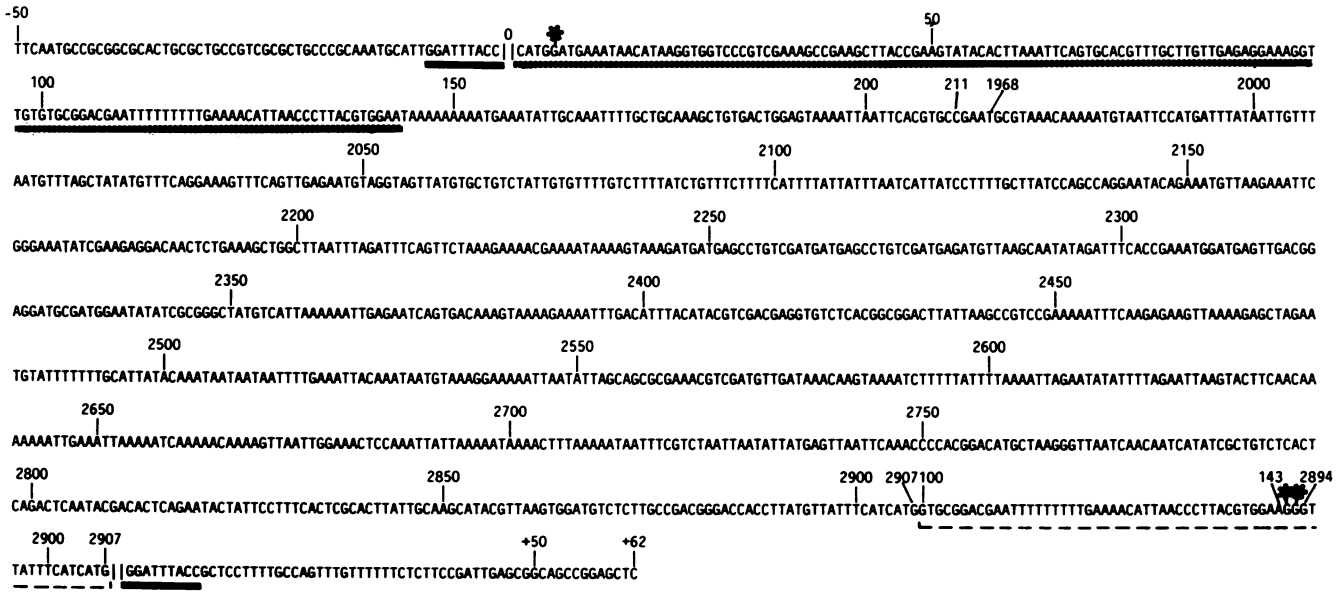

FIG. 7. DNA sequence analysis of $vg^{21\text{-}7\text{-}Rev}$. (A) Schematic representation, derived from sequencing, of the event that produced $vg^{21\text{-}7\text{-}Rev}$. (B) DNA sequence of $vg^{21\text{-}7\text{-}Rev}$. P-element sequences of $vg^{21\text{-}7}$ origin are indicated by a dashed line, while a hatched line denotes P-element DNA derived from either $vg^{21\text{-}7}$ or $vg^{21\text{-}7\text{-}Rev}$. The 9-bp duplication of the flanking *vg* region DNA is indicated with a solid bar, while asterisks indicate the extra bases seen in both $vg^{21\text{-}7}$ and $vg^{21\text{-}7\text{-}Rev}$ that differed from the published sequence (24), which was used for the numbering in this figure. The 3 bp at the junction of the internal deletion at positions 211 to 1968 are unlabeled since they correspond to nucleotides at positions 212 to 214 and 1965 to 1967 in the published sequence.

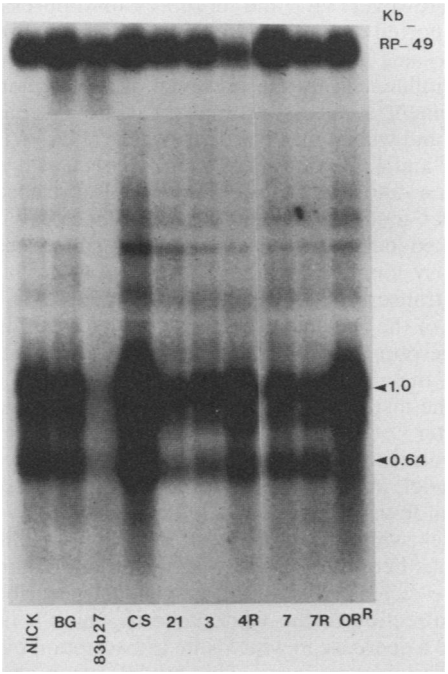

FIG. 8. Effects of P-element inserts on *vg* expression. A Northern blot of adult poly(A)$^+$ RNA from flies of the indicated genotypes was hybridized with a *vg* antisense RNA probe made from the restriction fragment indicated in Fig. 1. Size markers (data not shown) were *D. melanogaster* rRNA and mouse β-globin mRNA. A duplicate blot was probed with an oligolabeled ribosomal protein gene probe (RP49), to allow rough quantification of the amount of RNA loaded in each lane (23). The results of this second hybridization are shown at the top of the figure. The mutant alleles are labeled as described in the legend to Fig. 2, and NICK represents vg^{ni} (a spontaneous derivative of vg^{BG}), while CS denotes Canton-S (a wild-type strain).

DISCUSSION

Hybrid dysgenesis was used to induce a number of P-element alleles at the *vg* locus, and the molecular lesion associated with each allele was characterized. These mutations were derived from one P-element-induced parent allele (vg^{21}) by loss of internal P-element sequences, loss of adjacent genomic *vg* sequences, loss of the entire original P-element insert and flanking genomic sequences, or from insertion of additional sequences into the original P-element insert. There are a number of precedents for the first three types of alterations. P-element internal deletions have been observed by many investigators (4, 30, 34). Searles et al. (30), based on their sequence data of revertants of a P-element-induced RPII215 allele, speculated that internal deletions may preferentially originate in the P-element terminal repeats. The two internal deletion alleles sequenced here are consistent with this theory. The $vg^{21\text{-}4\text{-}Rev}$-specific deletion begins 13 bp into the 5′-terminal repeat, while the deletion associated with $vg^{21\text{-}7}$ starts 14 bp internal to the 3′-terminal repeat (Fig. 5), implying that the mechanisms in the generation of these deletions and the ones observed above are similar (30). Results for the $vg^{21\text{-}4}$ deletion were similar to these examples, except that the mutant deleted 36 bp of genomic *vg* DNA precisely from the end of the 3′-terminal repeat (Fig. 5). This type of deletion may be conceptually similar to the larger deletions reported previously (4, 34). However, since the previous examples were analyzed only at the restriction map level, we cannot be sure of this. These examples demonstrate that the terminal repeats can stimulate both internal and external deletions. Larger deletions similar to those seen with $vg^{21\text{-}9}$ and $vg^{21\text{-}12}$ are relatively common (4, 7, 34) and represent another consequence of aberrant P-element excision. Thus, these three classes of vg^{21} alleles were derived from predictable classes of putative P-element aberrant excision or transposition events.

The fourth class of vg^{21} derivatives includes those alleles caused by further insertions into extant P-element sequences. Although not yet sequenced, the results of the $vg^{21\text{-}3}$ analyses are consistent only with further insertion of P- element sequences into the vg^{21} P-element insert. The restriction map predicts that this insert may have resulted from gene conversion or recombination between a large P element (the $vg^{21\text{-}3}$ element) and the vg^{21} insert. Alternatively, the vg^{21} insert may have been excised and the larger $vg^{21\text{-}3}$ insert integrated at the same site (W. Engels, personal communication). These alternatives are currently being tested by sequencing the $vg^{21\text{-}3}$ insert. The second example of further insertion within a P-element insert is $vg^{21\text{-}7\text{-}Rev}$. This allele was caused by the insertion of approximately 1 kb of the P element DNA sequence into the residual 158 bp of P element sequence found in $vg^{21\text{-}7}$; by P- element integration at the 3′ end (at base 100 of $vg^{21\text{-}7}$) and what appears to be homologous recombination at the 5′ end. Conversely, this could have been generated by deletion of the 5′ end of $vg^{21\text{-}7}$ up to base 100, followed by integration of the $vg^{21\text{-}7\text{-}Rev}$ element into the remaining portion of the $vg^{21\text{-}7}$ element. Thus, we observed two separate examples of P-element insertions into preexisting P-element sequences. Since $vg^{21\text{-}6}$ is very similar to $vg^{21\text{-}3}$, it appears that three of the nine derivatives of vg^{21} described here are due to secondary insertions. Interestingly, one of these insertions was isolated as a revertant allele ($vg^{21\text{-}7\text{-}Rev}$), while the other was isolated as a phenotypically more extreme allele ($vg^{21\text{-}3}$). Secondary insertions of P elements into the region of existing P elements have also been observed at the yellow and singed loci (W. Eggleston and W. R. Engels, personal communication) and the *Sxl* locus (28a). However, these insertions have not been characterized in detail. The examples reported here may be similar to the homologous recombination events reported for the *D. melanogaster* retrotransposons that are involved in transpositional memory (21), or the unusual double transposons observed with the Ac-Ds controlling elements in maize (5). Conversely, they may represent examples of simultaneous ecision and insertion of P elements. The presence of an extra base in the 5′-terminal repeat of vg^{21} and all its sequenced derivatives argues that homologous recombination may be involved. If the $vg^{21\text{-}7}$ 5′ end was excised and replaced with another P element, it would be expected that the derivative would not have the extra base in the terminal repeat. Furthermore, if the $vg^{21\text{-}7\text{-}Rev}$ insert was due to an integration event at both the 5′ and 3′ ends, an 8-bp duplication should flank the 1.1-kb insert. The observation that the 8 bp at the 3′ end of the $vg^{21\text{-}7\text{-}Rev}$ insert (i.e., positions 100 to 107 in Fig. 7) were not duplicated at the other end of the element also argues that homologous recombination occurred at the 5′ end of the element. More alleles must be isolated and sequenced to determine the extent of the roles of homologous recombination and integration in the mechanisms of secondary insertion.

During the initial cloning of the locus, only one insert in 2 $\times$ 10^6 dysgenic flies was found (Williams and Bell, submitted). Thus, secondary insertions at the vg^{21} insertion site are

several hundred-fold more prevalant than the primary insertion event. This is likely to be due to the presence of P-element sequences at the vg^{21} site, since all of the alleles were derived from the same progenitor stock (OR-R), and the same P-cytotype stock ($\pi 2$) was used for both primary and secondary dysgenic crosses. Further alleles will have to be characterized to assay the mechanism and prevalence of secondary insertions. It is interesting that this class of P-element secondary insertion is so prevalent at *vg* but is rarely identified at other loci where similar types of analyses have been done (3, 30, 34, 35). Coding region insertions are unlikely to be reverted or enhanced by this type of mutation, perhaps explaining why secondary insertions have not been observed for these types of P-element mutants (i.e., white locus [24]). Experiments similar to those reported here have been conducted on P- element insertion mutants into noncoding sequences at the RPII215 (30, 35), rudimentary (33, 34), and yellow (3) loci. These alleles were all within the 5'-promoter-regions of the respective genes, while the vg^{21} insert was in the 3' region, at least with respect to adult *vg* transcription. It is possible that secondary insertion mutants are not as detectable within the physical environment of the promoter because of potentially different mechanisms by which P-element inserts in promoters disrupt gene function.

The effects of the recessive viable P-element-induced alleles on *vg* transcription were determined. These alleles were shown to reduce the level, but not the size, of adult *vg* transcripts. However, we can not be sure that the inserts disrupted *vg* expression the same way in the earlier stages of development, when the wing phenotype was determined. A more detailed examination of the relationship between *vg* phenotype and the quantitative reduction of *vg* transcription will be presented elsewhere (J. A. Williams and J. B. Bell, manuscript in preparation). Since all of these alleles contain insertions at the same genomic site and differ from each other only by what internal P-element sequences are present (except for $vg^{21\text{-}4}$), these sequenced alleles should provide an excellent opportunity to examine how P-element sequences can interfere with gene function.

The P-element inserts map in the 3' region of the *vg* gene, as assayed by the *vg* adult transcription unit (Williams and Bell, submitted; Williams and Bell, in preparation) and are transcribed antiparallel to *vg* transcription. Since all of the inserts are at the same genomic site and do not cause an alteration in transcript size, insertional interruption of the coding sequences is unlikely. Termination of *vg* transcription within the P-element inserts is also unlikely, since additional sequences are inserted in a complete revertant ($vg^{21\text{-}7\text{-}Rev}$) without any of the sequences present in the more phenotypically extreme parent allele ($vg^{21\text{-}7}$) being removed or altered. The same rationale makes *vg* splicing or polyadenylation within the P-element inserts unlikely. Furthermore, examination of DNA sequences within the sequenced P-element inserts shows no putative polyadenylation sites in the same orientation as *vg* transcription.

It is possible that P-element products may be involved in determining the severity of the mutants. In this model, the P-element products (i.e., the P-element repressor) would bind to specific P-element sequences and either enhance or suppress *vg* transcript levels by an unknown process. This was tested by crossing males of each allele to a multiply marked *vg* chromosome (in either a P or a M cytotype) and observing changes in phenotype over several generations. In fact, four *vg* alleles (vg^{21}, $vg^{21\text{-}3}$, $vg^{21\text{-}6}$, and $vg^{21\text{-}7\text{-}Rev}$) were shown to be dependent on the absence of repressor-producing P elements for their mutant phenotype to be expressed. However, vg^{21} and its repressor-suppressed derivatives reported in this study were all analyzed in a nonsuppressing genetic background; thus, their phenotypes were not influenced by the presence of a P-element repressor. P-element suppression appears to be a separate phenomenon and will be discussed elsewhere (J. A. Williams, S. S. Pappu, and J. B. Bell, Mol. Gen. Genet., in press).

Parkhurst and Corces (25) proposed a transcriptional interference model to explain the action of gypsy insertions at the forked locus. They speculated that enhancer elements in the gypsy long terminal repeat can act at a distance and suppress transcription from the forked promoter. The fact that none of the P-element-derived *vg* alleles discussed here caused aberrant *vg* transcripts is consistent with their model. However, the absence of a well-defined P-element enhancer (17) and the distance of the P-element inserts from the adult *vg* promoter (>6 kb) makes this explanation unlikely for the vg^{21} derivatives. Also, the results for $vg^{21\text{-}7\text{-}Rev}$ are contrary to this model, since the revertant had additional sequences rather than fewer.

A model which is consistent with the results of our analysis has been proposed by Bingham and Chapman (2). They have suggested that a transposon transcribed in the opposite direction to the white gene in which it is inserted may cause a decrease in white gene transcription by collision of transcription complexes. This model, when applied to P elements, would implicate two regions of P-element sequences in the disruption of the target gene function. The presence of a P-element promoter would cause a more extreme *vg* phenotype because of P-element transcription, while the presence of a transcription terminator would lead to a less extreme *vg* phenotype since the P-element transcripts would be shorter and less likely to interfere with *vg* transcription. In this model, the vg^{21} allele which has promoter and terminator sequences present (17) produces short P-element transcripts in adult flies (17) which interfere with productive *vg* transcription, causing a cryptic phenotype. Since the truncated *vg* transcripts would probably not be poly(A)$^+$, it is likely that they would be unstable and thus would not be detected by Northern analyses. The $vg^{21\text{-}7}$ allele produces a more extreme phenotype because of longer P-element transcripts, since the P-element terminator sequences have been deleted (17). These longer transcripts would be more likely to interfere with *vg* transcription. The $vg^{21\text{-}4}$ allele would have the same cryptic phenotypic effect as vg^{21} since it contains the same P-element sequences, but it is a more extreme mutant due to the loss of some genomic *vg* sequences. The $vg^{21\text{-}4\text{-}Rev}$ allele would be reverted since the P-element promoter region has been deleted (17). However, $vg^{21\text{-}4\text{-}Rev}$ is not a complete reversion since it still has the 36-bp deletion of genomic *vg* DNA which made $vg^{21\text{-}4}$ more extreme than vg^{21}. This model can also account for the revertant phenotype of $vg^{21\text{-}7\text{-}Rev}$ as being due to the restoration of the P-element terminator sequences by the extra insertion in $vg^{21\text{-}7\text{-}Rev}$. The model does not explain why $vg^{21\text{-}7\text{-}Rev}$ is less extreme than vg^{21}. Careful quantification of the levels of *vg* transcription for each allele is also required, to determine whether the reduction of transcription is rigorously correlated with the severity of *vg* phenotypes. In addition, *vg* expression during larval stages will have to be analyzed to establish whether the changes in RNA levels seen in adults reflect the effects seen earlier in development, when the wing phenotype is formed. However, the results presented here provide evidence for models in which transcription per se, within a transposable element, can interfere with target gene function.

ACKNOWLEDGMENTS

This study was supported by grant A9704 from the Natural Sciences and Engineering Research Council (Ottawa, Ontario, Canada) (to J. B. Bell) and predoctoral fellowship RA2603 (to J. A. Williams) from AHFMR.

We acknowledge Tove Reece for competent assistance in the preparation of the figures and R. B. Hodgetts for a critical reading of the manuscript. In addition, we acknowledge W. R. Engels for useful discussions.

LITERATURE CITED

1. **Bingham, P., R. Levis, and G. M. Rubin.** 1981. Cloning of DNA sequences from the white locus of *D. melanogaster* by a novel and general method. Cell **25**:693–704.
2. **Bingham, P. M., and C. H. Chapman.** 1986. Evidence that white-blood is a novel type of temperature sensitive mutation resulting from temperature-dependent effects of a transposon insertion on formation of white transcripts. EMBO J. **5**:3343–3352.
3. **Chia, W., G. Howes, M. Martin, Y. B. Meng, K. Moses, and S. Tsubota.** 1986. Molecular analysis of the yellow locus of *Drosophila*. EMBO J. **5**:3597–3605.
4. **Daniels, S. B., M. McCarron, C. Love, and A. Chovnick.** 1985. Dysgenesis-induced instability of rosy locus transformation in *Drosophila melanogaster*: analysis of excision events and the selective recovery of control element deletions. Genetics **109**: 95–117.
5. **Doring, H. P., E. Tillmann, and P. Starlinger.** 1984. DNA sequence of the maize transposable element dissociation. Nature (London) **307**:127–130.
6. **Engels, W. R.** 1983. The P family of transposable elements in *Drosophila*. Annu. Rev. Genet. **17**:315–344.
7. **Engels, W. R., and C. R. Preston.** 1981. Identifying P factors in *Drosophila* by means of chromosome breakage hotspots. Cell **26**:421–428.
8. **Feinberg, A. P., and B. Vogelstein.** 1983. A technique for radiolabeling DNA restriction endonuclease fragments to high specific activity. Anal. Biochem. **132**:6–13.
9. **Frischauf, A., H. Lehrach, A. Poustka, and N. Murray.** 1983. Lambda replacement vectors carrying polylinker sequences. J. Mol. Biol. **170**:827–842.
10. **Fristrom, D.** 1969. Cellular degeneration in the production of some mutant phenotypes in *Drosophila melanogaster*. Mol. Gen. Genet. **103**:363–379.
11. **Gietz, R. D., and R. B. Hodgetts.** 1985. An analysis of dopa decarboxylase expression during embryogenesis in *Drosophila melanogaster*. Dev. Biol. **107**:142–155.
12. **Hoopes, B. C., and W. R. McClure.** 1981. Studies on the selectivity of DNA precipitation by spermine. Nucleic Acids Res. **9**:5493–5505.
13. **Ish-Horowicz, D., S. M. Pinchin, P. Schedl, S. Artavanis-Tsakonas, and M. Mirault.** 1979. Genetic and molecular analysis of the 87A7 and 87C1 heat-inducible loci of *D. melanogaster*. Cell **18**:1351–1358.
14. **Karess, R. E., and G. M. Rubin.** 1984. Analysis of P-transposable element functions in *Drosophila*. Cell **38**:135–146.
15. **Kelley, M. R., S. Kidd, R. V. Berg, and M. W. Young.** 1987. Restriction of P-element insertions at the notch locus of *Drosophila melanogaster*. Mol. Cell. Biol. **7**:1545–1548.
16. **Klessig, D., and J. O. Berry.** 1983. Improved filter hybridization method for detection of single copy sequences in large eukaryotic genomes. Plant Mol. Biol. Rep. **I**:12–18.
17. **Laski, F. A., D. C. Rio, and G. M. Rubin.** 1986. Tissue specificity of *Drosophila* P-element transposition is regulated at the level of mRNA splicing. Cell **44**:7–19.
18. **Maine, E. M., H. K. Salz, T. W. Cline, and P. Schedl.** 1985. The sex-lethal gene of *Drosophila*: DNA alterations associated with sex-specific lethal mutations. Cell **43**:521–529.
19. **Maniatis, T., E. F. Fritsch, and J. Sambrook.** 1982. Molecular cloning: a laboratory manual. Cold Spring Harbor Laboratory, Cold Spring Harbor, N.Y.
20. **Melton, D. A., P. A. Krieg, M. R. Rebagliati, T. Maniatis, K. Zinn, and M. R. Green.** 1984. Efficient in vitro synthesis of biologically active RNA and RNA hybridization probes from plasmids containing a bacteriophage SP6 promotor. Nucleic Acids Res. **12**:7035–7055.
21. **Mizrokhi, L. J., L. A. Obolenkova, A. F. Priimagi, Y. V. Ilyin, T. I. Gerasimova, and G. P. Georgiev.** 1985. The nature of unstable insertion mutations and reversions in the locus cut of *Drosophila melanogaster*: molecular mechanism of transposition memory. EMBO J. **4**:3781–3787.
22. **Nash, D., and J. B. Bell.** 1968. Larval age and the pattern of DNA synthesis in polytene chromosomes. Can. J. Genet. Cytol. **10**:82–92.
23. **O'Connell, P., and M. Rosbach.** 1984. Sequence, structure and codon preference of the *Drosophila* ribosomal protein 49 gene. Nucleic Acids Res. **12**:5495–5513.
24. **O'Hare, K., and G. M. Rubin.** 1983. Structures of P transposable elements and their sites of insertion and excision in the *Drosophila melanogaster* genome. Cell **34**:25–35.
25. **Parkhurst, S. M., and V. G. Corces.** 1985. Forked, gypsys and suppressors in *Drosophila*. Cell **41**:429–437.
26. **Rio, D. C., F. A. Laski, and G. M. Rubin.** 1986. Identification and immunochemical analysis of biologically active *Drosophila* P element transposase. Cell **44**:21–32.
27. **Rubin, G. M., M. G. Kidwell, and P. M. Bingham.** 1982. The molecular basis of P-M hybrid dysgenesis: the nature of induced mutations. Cell **29**:987–994.
28. **Rubin, G. M., and A. C. Spradling.** 1982. Genetic transformation of *Drosophila* with transposable element-vectors. Science **218**:348–353.

28a. **Salz, H. K., T. W. Cline, and P. Schedl.** 1987. Functional changes associated with structural alterations induced by mobilization of a P element inserted in the Sex-lethal gene of *Drosophila*. Genetics **117**:221–231.

29. **Sanger, F., S. Nicklen, and A. R. Coulson.** 1977. DNA sequencing with chain terminating inhibitors. Proc. Natl. Acad. Sci. USA **74**:5463–5467.
30. **Searles, L. L., A. L. Greenleaf, W. E. Kemp, and R. A. Voelker.** 1986. Sites of P element insertion and structures of P element deletions in the 5′ region of *Drosophila melanogaster* RepII215. Mol. Cell. Biol. **6**:3312–3319.
31. **Searles, L. L., R. Jokerst, P. Bingham, R. Voelker, and A. L. Greenleaf.** 1982. Molecular cloning of sequences from a *Drosophila* DNA polymerase II locus by P element transposon tagging. Cell **31**:585–592.
32. **Spradling, A. C., and G. M. Rubin.** 1982. Transposition of cloned P elements into *Drosophila* germ line chromosomes. Science **281**:341–347.
33. **Tsubota, S., M. Ashburner, and P. Schedl.** 1985. P-element-induced control mutations at the r gene of *Drosophila melanogaster*. Mol. Cell. Biol. **5**:2567–2574.
34. **Tsubota, S., and P. Schedl.** 1986. Hybrid dysgenesis-induced revertants of insertion at the 5′ end of the rudimentary gene in *Drosophila melanogaster*: transposon-induced control mutations. Genetics **114**:165–182.
35. **Voelker, R. A., A. L. Greenleaf, H. Gyurkovics, G. B. Wisely, S. Huang, and L. L. Searles.** 1984. Frequent imprecise excision among reversions of a P element-caused lethal mutation in *Drosophila*. Genetics **107**:279–294.